Ab Initio Calculations on $H + C_2H_2 \rightarrow C_2H_3$ Using Unrestricted Møller–Plesset Perturbation Theory with Spin Projection

CARLOS SOSA* AND H. BERNHARD SCHLEGEL†
Department of Chemistry, Wayne State University, Detroit, Michigan, 48202

Abstract

Hydrogen addition to acetylene has been studied by molecular orbital methods with the unrestricted Hartree–Fock (HF) approach and with Møller–Plesset (MP) perturbation theory up to fourth order using the 6-31G*, 6-31G**, and 6-311G** basis sets. For each basis set a number of points along an approximate reaction path were calculated by fixing the attacking H—C distance and optimizing all of the remaining parameters. At these geometries, single point MP4 calculations with and without spin projection were carried out, yielding the position, height, and shape of the addition barrier at the various levels of calculation with each of the three basis sets. The results of this approach were confirmed by a grid search of the region near the transition state using the 6-31G* basis set. The unprojected MP2, MP3, and MP4 barriers are too narrow and are 10–20 kcal/mol too high. With spin projection, the barriers are much lower and broader. At the PMP4SDTQ/6-311G** level, with zero point energy calculated at UHF/6-31G*, the vibrationally adiabatic barrier at 0 K is 4.0 kcal/mol, and the attacking H—C distance is 2.0 Å.

Introduction

The addition of atomic hydrogen to C_2H_2 is one of the important reactions in acetylene flames and has been the subject of numerous experimental and theoretical studies (Refs. 1–7; for recent reviews of $H + C_2H_2$ addition, see Refs. 8–10). One of the difficulties of interpreting $H + C_2H_2 \rightleftharpoons C_2H_3$ is that different activated complexes appear to be needed to explain the forward and reverse reactions [5, 6, 10]. The experimental activation energy for the addition reaction is 2.4–2.7 kcal/mol [1–3], and the heat of reaction has been estimated to be $\Delta H(298\ \text{K}) = -35.8$ kcal/mol [11]. Early theoretical studies on this system included unrestricted Hartree–Fock calculations with a 4-31G basis [7]. The most extensive calculations to date on the transition state for $H + C_2H_2$ have been at the POL-CI level with a double-zeta plus polarization basis set [10] and yield 8.3 kcal/mol for the addition barrier and −29.1

*Present address: Quantum Theory Project, University of Florida, Gainesville, Florida 32605.
†Camille and Henry Dreyfus Teacher-Scholar.

INTERNATIONAL JOURNAL OF QUANTUM CHEMISTRY: QUANTUM CHEMISTRY SYMPOSIUM 21, 267–282 (1987)
 CCC 0360-8832/87/210267-16$04.00

kcal/mol for $\Delta H(0\ K)$ [10]. A more reliable theoretical estimate of the heat of reaction has been obtained by MP4/6-31G** calculations with bond additivity corrections [12] (BAC-MP4/6-31G**), which give $\Delta H(0\ K) = -35.5$ kcal/mol and $\Delta H(298\ K) = -36.7$ kcal/mol.

In previous calculations on $H + C_2H_4 \rightleftharpoons C_2H_5$, $H + CH_2O \rightleftharpoons CH_3O$ [13] and $OH + C_2H_{2n} \rightleftharpoons HOC_2H_{2n}$ [14], barriers computed by Møller–Plesset perturbation theory based on an unrestricted Hartree–Fock reference determinant were found to be 5–10 kcal/mol too high because of serious spin contamination problems. Spin contamination also causes severe convergence difficulties in Møller–Plesset perturbation calculations of bond dissociation potentials [15–18]. When the largest spin contaminants are annihilated, the heights of barriers and the shapes of potential energy curves are greatly improved [13, 18]. In the present paper, these spin annihilation techniques are applied to $H + C_2H_2 \rightleftharpoons C_2H_3$.

Method

Ab initio molecular orbital calculations were performed with the GAUSSIAN 82 system of programs [19] using the 6-31G*, 6-31G**, and 6-311G** basis sets [20]. Electron correlation corrections were estimated by Møller–Plesset perturbation theory [21][†] up to fourth order (MP2, MP3, MP4, frozen core). Unwanted spin contamination was removed using projection methods [18] (PMP2, PMP3, PMP4, see below). Equilibrium geometries and transition structures were optimized at the UHF level with each of the basis sets using analytical gradient methods [23].

For the spin projected post-Hartree–Fock calculations, complete optimization was not practical because analytical gradients have not yet been programmed. Instead, two approximate methods were used to estimate the positions of the transition structure for the various levels of calculation with electron correlated and spin projection. In the first approach, several points along an approximate reaction path were obtained by fixing the C—H distance for the attacking hydrogen, R(CH*), and optimizing all of the remaining parameters at the Hartree–Fock level with each of the three basis sets. Single point calculations with correlation corrections and spin projection were carried out at each of these points to yield a series of potential energy profiles along the approximate reaction path. In the second approach, a coarse grid was used to explore the region of the transition state at the MP*n*/6-31G* level with and without spin projection. Since the variations in the CH bond lengths along the reaction path were found to be small, the R(CH)'s were fixed at 1.06955 Å, obtained from the MP4SDTQ/6-31G* optimization of C_2H_2 [24]. The step sizes for the grid were 0.02 Å for R(CC), 5° for the angles, and 0.1 Å for R(CH*). A total of 59 calculations yielded numerical gradients and diagonal second derivatives at 6 points on the potential energy surface. The numerical gradients at these points were combined with the Hartree–Fock analytical second derivative matrix calculated at the HF transition state[‡]

[†]For a review of many body perturbation theory and coupled cluster methods, see Ref. 22.

[‡]Since the numerical calculation of the second derivatives indicated that the diagonal R(CC) and R(CH*) stretching force constants calculated at the MP*n* and PMP*n* levels are consistently larger than the Hartree–Fock values, 1.2 and −0.02 a.u. were used instead of 0.79 and −0.012 a.u.

to predict the location and energy of the transition state. For each level of calculation, the final estimate is based on the gradients calculated at the grid point closest to the predicted transition structure.

In the region of the transition structure, the unrestricted Hartree–Fock calculations suffer serious problems with spin contamination, i.e., $\langle\Psi_0|\hat{S}^2|\Psi_0\rangle \neq s(s+1)$. When correlation corrections are included, $\hat{S}^2$ can be calculated as $\langle\Psi_0|\hat{S}^2|\Psi_0+\Psi_1\rangle$, $\langle\Psi_0|\hat{S}^2|\Psi_0+\Psi_1+\Psi_2\rangle$, etc., where Ψ_1, Ψ_2, etc., are the first, second, and higher order correction to the wave function. However, correlation corrections obtained by Møller–Plesset perturbation theory do not improve the spin contamination problem significantly [18]. Alternatively, the unwanted spin contaminants can be removed by using the Löwdin spin projection operator [25].

$$\hat{P}_s = \prod_{k\neq s} \frac{\hat{S}^2 - k(k+1)}{s(s+1) - k(k+1)} \tag{1}$$

This series converges rapidly, and only the largest 2 or 3 spin contaminants need to be annihilated. The projected Hartree–Fock energy can be written as

$$E_{\text{PUHF}} = \langle\hat{P}_s\Psi_0|\hat{H}|\hat{P}_s\Psi_0\rangle/\langle\hat{P}_s\Psi_0|\hat{P}_s\Psi_0\rangle = \langle\Psi_0|\hat{H}\hat{P}_s|\Psi_0\rangle/\langle\Psi_0|\hat{P}_s|\Psi_0\rangle \tag{2}$$

$$= \langle\Psi_0|\hat{H}|\Psi_0\rangle + \sum_{i\neq 0}\frac{\langle\Psi_0|\hat{H}|\psi_i\rangle\langle\psi_i|\hat{P}_s|\Psi_0\rangle}{\langle\Psi_0|\hat{P}_s|\Psi_0\rangle} = E_{\text{HF}} + \Delta E_{\text{PUHF}}$$

Because the UHF wave function satisfies Brillouin's theorem, and $\hat{H}$ contains only 1- and 2-electron operators, the summation can be restricted to double excitations. The spin-projected UHF wave function (in intermediate normalization) can be written as the ground state determinant plus contributions from single, double, and higher excited determinants.

$$\hat{P}_s\Psi_0/\langle\Psi_0|\hat{P}_s|\Psi_0\rangle = \Psi_0 + \tilde{\Psi}_1 + \text{higher excitations} \tag{3}$$

where $\tilde{\Psi}_1$ contains all of the contributions from the single and double excitations,

$$\tilde{\Psi}_1 = \sum_i^{s,d} \psi_i\langle\psi_i|\hat{P}_s|\Psi_0\rangle/\langle\Psi_0|\hat{P}_s|\Psi_0\rangle \tag{4}$$

Without approximations, the projected Hartree–Fock energy can be expressed as

$$E_{\text{PUHF}} = \langle\Psi_0|\hat{H}|\Psi_0\rangle + \langle\Psi_0|\hat{H}|\tilde{\Psi}_1\rangle \tag{5}$$

Since electron correlation energies with spin projection are difficult to calculate directly, two approximations are made: (1) only single and double excitations are considered for the spin projection corrections to Ψ_0, and (2) the spin projection corrections, $\tilde{\Psi}_1$, are reduced by the amount already contained in the correlation corrections, Ψ_1, Ψ_2, etc. These approximations have been used successfully in previous calculations where only the largest spin contaminant was annihilated [13, 14, 18]. The approximate projected MP2, MP3, and MP4 energies used in the present calculations are

$$E_{\text{PMP2}} = E_{\text{MP2}} + \Delta E_{\text{PUHF}}\{1 - \langle\Psi_1|\tilde{\Psi}_1\rangle/\langle\tilde{\Psi}_1|\tilde{\Psi}_1\rangle\} \tag{6}$$

$$E_{\text{PMP3}} = E_{\text{MP3}} + \Delta E_{\text{PUHF}}\{1 - \langle\Psi_1+\Psi_2|\tilde{\Psi}_1\rangle/\langle\tilde{\Psi}_1|\tilde{\Psi}_1\rangle\} \tag{7}$$

$$E_{PMP4} = E_{MP4} + \Delta E_{PUHF}\{1 - \langle \Psi_1 + \Psi_2 + \Psi_3 | \tilde{\Psi}_1 \rangle / \langle \tilde{\Psi}_1 | \tilde{\Psi}_1 \rangle\}$$
$$\approx E_{MP4} + \Delta E_{PUHF}\{1 - \langle \Psi_1 + \Psi_2 | \tilde{\Psi}_1 \rangle / \langle \tilde{\Psi}_1 | \tilde{\Psi}_1 \rangle\} \quad (8)$$

where $\tilde{\Psi}_1$ contains the single and double excitations arising from the annihilation of all spin contaminants contributing more than 10^{-6} a.u. to the energy.

Harmonic vibrational frequencies were computed at the UHF/6-31G* level using analytical second derivatives [26] (no scaling). Partition functions and thermal corrections were calculated using standard methods in statistical mechanics [27] (298 K, 1 atm). For structures other than the reactants and products, the vibrational mode corresponding to the reaction coordinate was not included.

Results and Discussion

Tables I–III list the geometries and relative energies of points along the approximate reaction path computed with the 6-31G*, 6-31G**, and 6-311G** basis sets. The geometrical parameters are defined in Figure 1. The variations of the bond lengths and angles along the reaction path computed at the UHF/6-311G** level are illustrated in Figure 2; the data for the other basis sets are very similar. For the C_2H_2 fragment, the CC bond length and the CCH angles undergo the largest changes. The changes are relatively small between the reactants and the transition state; most of the changes in the geometrical parameters occur between the transition structure and the products. Nevertheless, the greatest rate of change of the geometry is in the vicinity of the transition state.

The energy profiles along the approximate reaction path are shown in Figures 3–5 for the 6-31G*, 6-31G**, and 6-311G** basis sets. In each case, zero point energy has been included at the UHF/6-31G* level. The Hartree–Fock potential energy curves are quite similar; each has a low, broad barrier near 1.9 Å. For the UHF/6-31G* and UHF/6-31G** curves, the barrier is 6.2–6.3 kcal/mol, and the exothermicity is 41–42 kcal/mol; when the basis set is enlarged to 6-311G**, the barrier increases by 1 kcal/mol, and the exothermicity is reduced by 3 kcal/mol.

In contrast to the Hartree–Fock calculations, the potential energy curves at the MP2, MP3, and MP4 levels have high, narrow barriers that are shifted 0.1–0.2 Å closer

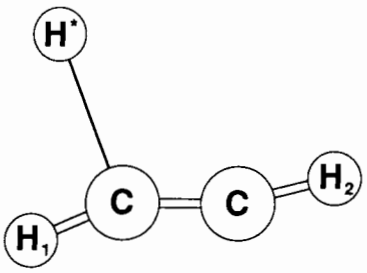

Figure 1. Definition of geometrical parameters for points along the approximate reaction path for $H + C_2H_2 \rightarrow C_2H_3$.

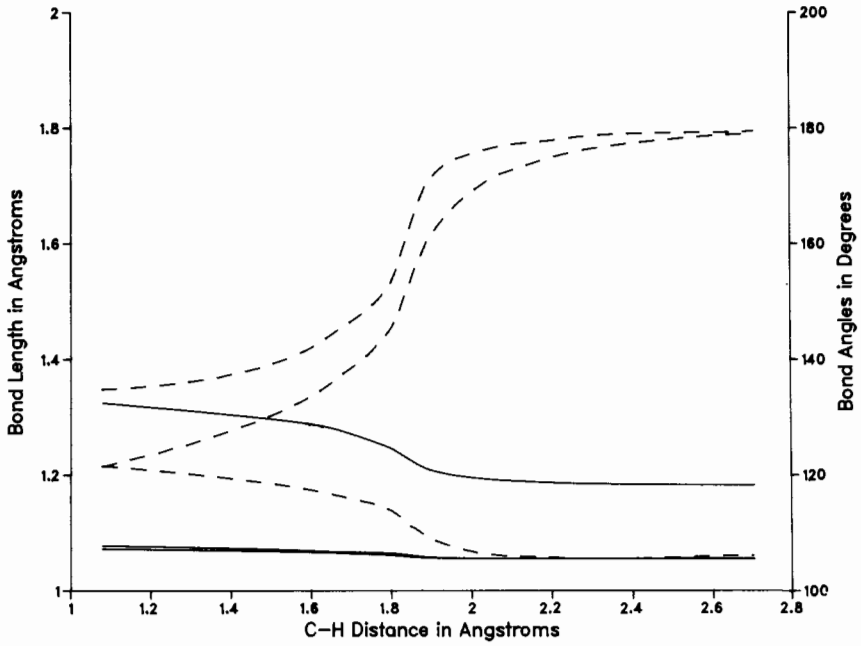

Figure 2. Variation of the bond lengths (solid lines) and bond angles (dashed lines) along the approximate reaction path for H + $C_2H_2 \rightarrow C_2H_3$ (6-311G** basis set).

to the products. The barrier heights, 10–25 kcal/mol, are far too large because of substantial spin contamination ($\langle\Psi_0|\hat{S}^2|\Psi_0\rangle \gg 0.75$). Correlation corrections do little to reduce the spin contamination ($\langle\Psi_0|\hat{S}^2|\Psi_0 + \Psi_1\rangle$, $\langle\Psi_0|\hat{S}^2|\Psi_0 + \Psi_1 + \Psi_2\rangle \approx \langle\Psi_0|\hat{S}^2|\Psi_0\rangle$, Tables I–III).[†] A comparison of the MP4SDQ and MP4SDTQ calculations with the 6-311G** basis set reveals that the contribution from the triple excitations is surprisingly large, reducing the exothermicity by 3.3 kcal/mol and raising the barrier by 2 kcal/mol at R(CH*) = 1.8 Å. However, the contribution from the triples diminished rapidly with R(CH*) elongation, dropping to less than 0.4 kcal/mol by R(CH*) = 2.0 Å.

When spin projection is included, the barrier height and shape change drastically. Compared with the MP4 calculations, the barriers at the PMP4 level are shifted about 0.1–0.2 Å toward H + C_2H_2 and have become very flat, even broader than the UHF barrier.[‡] At R(CH*) = 2.0 Å, the barrier is 3.7 kcal/mol at PMP4SDQ/6-311G** and 4.0 kcal/mol at PMP4SDTQ/6-311G** (ΔZPE computed at UHF/6-31G*). However, it should be noted that rate of change of the spin projection correction and the MP4 triples contribution are both quite large near R(CH*) = 2.0 Å, and further refine-

[†]After spin projection, $\langle S^2\rangle$ = 0.74–0.75 at the PMP*n* levels.

[‡]The residual shoulder in the PMP4 curves near 1.8 Å appears to be an artifact associated with the approximations made in determining the reaction path and/or calculating the spin projection at the correlated levels.

TABLE I. Geometries, vibrational frequencies, and energies along an approximate reaction path for H + HCCH computed with the 6-31G* basis set.

Geometrical parameters (Å and degrees)						
R(CH*)	1.0801	1.6000	1.7000	1.8000	1.9000	1.9178
R(CC)	1.3282	1.2934	1.2786	1.2596	1.2221	1.2162
$R(CH_1)$	1.0766	1.0685	1.0663	1.0640	1.0598	1.0589
$R(CH_2)$	1.0714	1.0664	1.0646	1.0623	1.0581	1.0577
<CCH*	121.82	117.91	116.64	115.05	111.06	110.15
$<CCH_1$	121.49	133.18	137.43	143.02	156.23	159.04
$<CCH_2$	134.35	140.82	144.57	150.29	165.91	168.55
Vibrational frequencies (cm^{-1})						
a'CH* stretch	3279	1666 i	1536 i	1305 i	1015 i	947 i
CCH* bend	1196	987	845	689	473	453
CCH bend	829	774	694	591	572	592
CCH bend	1634	1224	1095	971	879	878
CC stretch	1407	1554	1585	1641	1794	1827
CH stretch	3373	3467	3496	3525	3577	3585
CH stretch	3429	3501	3529	3565	3635	3646
a"CCH bend	885	782	687	619	647	665
CCH bend	959	853	821	799	807	814
Thermodynamic parameters (Kcal/mol, eu)						
ΔZPE	24.29	18.79	18.23	17.73	17.70	17.81
$E(298)-E(0)$	1.90	1.96	2.03	2.12	2.22	2.21
Entropy	55.67	56.34	56.70	57.19	57.60	57.59
ln (Q)	23.7605196	23.966721	23.994317	24.014596	23.997278	23.995734
Total energies (au)						
HF	−77.390292	−77.322759	−77.313352	−77.307476	−77.304922	−77.304875
MP2	−77.601847	−77.534890	−77.525095	−77.522470	−77.533678	−77.536217
MP3	−77.623994	−77.556850	−77.546125	−77.542131	−77.550024	−77.551870
MP4SDQ	−77.630553	−77.565974	−77.555401	−77.551324	−77.558230	−77.559763
PUHF	−77.403924	−77.348197	−77.341413	−77.334865	−77.323359	−77.321154
PMP2	−77.614152	−77.557515	−77.550116	−77.546895	−77.549828	−77.550422
PMP3	−77.634011	−77.575110	−77.566436	−77.561854	−77.562379	−77.562606
PMP4SDQ	−77.640570	−77.584234	−77.575712	−77.571047	−77.570585	−77.570499
Spin						
$\langle\Psi_0\|S^2\|\Psi_0\rangle$	1.0154	1.1773	1.2305	1.2216	1.0372	0.9987
$\langle\Psi_0\|S^2\|\Psi_0 + \Psi_1\rangle$	0.9890	1.1267	1.1746	1.1670	1.0002	0.9660
$\langle\Psi_0\|S^2\|\Psi_0 + \Psi_1 + \Psi_2\rangle$	0.9440	1.0489	1.0884	1.0808	0.9390	0.9115
Relative energies[a] (kcal/mol)						
HF	−40.77	−3.89	1.45	4.64	6.21	6.35
MP2	−18.65	17.86	23.45	24.60	17.53	16.05
MP3	−26.01	10.63	16.80	18.80	13.82	12.77
MP4SDQ	−27.02	8.01	14.08	16.14	11.77	10.92
PUHF	−49.33	−19.86	−16.16	−12.55	−5.36	−3.87
PMP2	−26.37	3.67	7.75	9.27	7.40	7.14
PMP3	−32.29	−0.83	4.05	6.43	6.07	6.04
PMP4SDQ	−33.30	−3.45	1.33	3.76	4.02	4.19

[a]Includes zero point energy calculated at the UHF/6-31G* level.

2.0000	2.1000	2.2000	2.3000	2.4000	2.5000	2.7000	infinite
1.2021	1.1947	1.1909	1.1886	1.1874	1.1886	1.1859	1.1855
1.0573	1.0566	1.0563	1.0563	1.0563	1.0564	1.0566	1.0570
1.0571	1.0570	1.0569	1.0570	1.0570	1.0570	1.0570	1.0570
107.57	106.31	105.74	105.51	105.93	105.85	106.13	—
167.03	171.76	174.48	176.17	177.21	178.03	178.99	180.00
174.14	176.54	177.75	178.45	178.90	179.2	179.59	180.00
640 i	256 i	328	420				0
336	286	224	179				0
678	732	758	774				794
884	883	881	883				883
1934	2023	2092	2146				2247
3601	3606	3609	3609				3607
3671	3687	3699	3706				3719
720	753	770	781				794
841	858	868	874				883
18.15	18.34	18.44	18.52	18.50	18.50	18.50	18.48
2.21	2.25	2.30	2.33				21.02
57.71	58.10	58.57	59.06				73.27
24.016676	24.060968	23.880777	24.019828				30.507192
−77.305505	−77.307028	−77.308683	−77.310208	−77.311518	−77.312594	−77.314136	−77.316059
−77.543544	−77.548999	−77.552882	−77.555711	−77.557755	−77.559227	−77.561052	−77.562864
−77.557182	−77.561323	−77.564425	−77.566778	−77.568836	−77.569842	−77.571519	−77.573292
−77.564064	−77.566747	−77.570110	−77.572163	−77.573738	−77.574931	−77.576506	−77.578237
−77.315516	−77.312998	−77.321271	−77.312339	−77.312771	−77.313325	−77.314382	−77.316059
−77.552203	−77.554142	−77.555967	−77.557539	−77.558830	−77.559852	−77.561261	−77.562864
−77.563516	−77.565013	−77.566612	−77.568066	−77.569290	−77.570279	−77.571664	−77.573292
−77.570398	−77.570437	−77.572297	−77.573451	−77.574192	−77.575368	−77.576651	−77.578237
0.8976	0.8373	0.8022	0.7809	0.7681	0.7604	0.7534	0.7500
0.8773	0.8250	0.7948	0.7765	0.7655	0.7589	0.7529	0.7500
0.8425	0.8036	0.7817	0.7686	0.7609	0.7562	0.7520	0.7500
6.29	5.53	4.59	3.71	2.87	2.19	1.23	0.00
11.79	8.56	6.22	4.53	3.23	2.30	1.16	0.00
9.78	7.37	5.52	4.13	2.82	2.18	1.13	0.00
8.56	7.07	5.06	3.85	2.84	2.09	1.11	0.00
0.01	1.78	2.34	2.37	2.08	1.74	1.07	0.00
6.36	5.33	4.29	3.38	2.55	1.91	1.03	0.00
5.80	5.06	4.15	3.32	2.53	1.91	1.04	0.00
4.59	4.75	3.69	3.04	2.56	1.82	1.02	0.00

TABLE II. Geometries and energies along an approximate reaction path for H + HCCH computed with the 6-31G** basis set.

Geometrical parameters (Å and degrees)						
R(CH*)	1.0801	1.6000	1.7000	1.8000	1.9214	2.0000
R(CC)	1.3278	1.2936	1.2788	1.2600	1.2157	1.2028
$R(CH_1)$	1.0771	1.0689	1.0688	1.0645	1.0589	1.0573
$R(CH_2)$	1.0721	1.0669	1.0650	1.0627	1.0576	1.0571
<CCH*	121.63	117.74	116.51	114.95	109.80	107.56
$<CCH_1$	121.36	133.06	137.45	143.01	159.68	167.06
$<CCH_2$	134.43	140.01	144.73	150.35	169.23	174.18
Total energies (au)						
HF	−77.395901	−77.327850	−77.318090	−77.311964	−77.309206	−77.309769
MP2	−77.625903	−77.555068	−77.544012	−77.540206	−77.553165	−77.559583
MP3	−77.649582	−77.577964	−77.565973	−77.560788	−77.569524	−77.574045
MP4SDQ	−77.655424	−77.586433	−77.574689	−77.569472	−77.576887	−77.580482
PUHF	−77.409481	−77.352981	−77.345939	−77.339236	−77.325042	−77.319836
PMP2	−77.638159	−77.577418	−77.568845	−77.564529	−77.566976	−77.568294
PMP3	−77.659550	−77.595944	−77.586071	−77.580389	−77.579924	−77.580413
PMP4SDQ	−77.665392	−77.604413	−77.594787	−77.589073	−77.587287	−77.586850
Spin						
$\langle\Psi_0\|S^2\|\Psi_0\rangle$	1.0140	1.1725	1.2274	1.2207	0.9920	0.8991
$\langle\Psi_0\|S^2\|\Psi_0 + \Psi_1\rangle$	0.9876	1.1225	1.1718	1.1662	0.9601	0.8786
$\langle\Psi_0\|S^2\|\Psi_0 + \Psi_1 + \Psi_2\rangle$	0.9427	1.0445	1.0851	1.0795	0.9065	0.8434
Relative energies[a] (kcal/mol)						
HF	−41.77	−4.57	0.99	4.34	6.15	6.13
MP2	−24.37	14.58	20.96	22.84	14.79	11.10
MP3	−31.64	7.80	14.76	17.52	12.12	9.62
MP4SDQ	−33.04	4.75	11.56	14.33	9.76	7.84
PUHF	−50.30	−20.34	−16.48	−12.78	−3.79	−0.18
PMP2	−32.06	0.55	5.37	7.58	6.13	5.64
PMP3	−37.90	−3.48	2.15	5.22	5.59	5.62
PMP4SDQ	−39.30	−6.53	−1.05	2.03	3.23	3.85

[a]Includes zero point energy calculated at the UHF/6-31G* level; see Table I.

2.1000	2.2000	2.3000	2.4000	2.5000	2.7000	infinite
1.1955	1.1916	1.1893	1.1881	1.1872	1.1865	1.1862
1.0566	1.0563	1.0563	1.0563	1.0563	1.0563	1.0569
1.0569	1.0569	1.0569	1.0569	1.0569	1.0569	1.0569
106.27	105.74	105.47	105.89	105.80	106.13	—
171.85	174.52	176.20	177.23	178.05	178.99	180.00
176.64	177.76	178.50	178.91	179.24	179.59	180.00
−77.311226	−77.312834	−77.314327	−77.315612	−77.316675	−77.318197	−77.320070
−77.564750	−77.568435	−77.571121	−77.573069	−77.574460	−77.576179	−77.577805
−77.577878	−77.580770	−77.582970	−77.584622	−77.585845	−77.587407	−77.589899
−77.583593	−77.586021	−77.587923	−77.589395	−77.590503	−77.591964	−77.593506
−77.317263	−77.316482	−77.316507	−77.316905	−77.317428	−77.318451	−77.320070
−77.569953	−77.571571	−77.572992	−77.574177	−77.575107	−77.576396	−77.577805
−77.581608	−77.582993	−77.584288	−77.585399	−77.586295	−77.587558	−77.589899
−77.587323	−77.588244	−77.589241	−77.590172	−77.590953	−77.592115	−77.593506
0.8386	0.8033	0.7818	0.7687	0.7608	0.7535	0.7500
0.8262	0.7958	0.7773	0.7661	0.7592	0.7530	0.7500
0.8044	0.7824	0.7692	0.7613	0.7564	0.7521	0.7500
5.41	4.50	3.64	2.82	2.15	1.20	0.00
8.05	5.84	4.23	2.99	2.12	1.04	0.00
7.40	5.69	4.39	3.33	2.56	1.58	0.00
6.08	4.66	3.54	2.60	1.90	0.99	0.00
1.62	2.21	2.28	2.01	1.68	1.04	0.00
4.79	3.87	3.06	2.30	1.71	0.90	0.00
5.06	4.29	3.56	2.84	2.28	1.49	0.00
3.74	3.26	2.72	2.11	1.62	0.89	0.00

TABLE III. Geometries and energies along an approximate reaction path for H + HCCH computed with the 6-311G** basis set.

Geometrical parameters (Å and degrees)					
R(CH*)	1.0801	1.6000	1.7000	1.8000	1.8836
R(CC)	1.3240	1.2874	1.2703	1.2447	1.2111
$R(CH_1)$	1.0774	1.0688	1.0664	1.0645	1.0582
$R(CH_2)$	1.0721	1.0664	1.0640	1.0610	1.0566
<CCH*	121.54	117.39	115.92	113.82	109.47
$<CCH_1$	121.47	133.69	138.60	145.61	159.89
$<CCH_2$	134.81	142.09	146.67	153.59	170.12
Total energies (au)					
HF	−77.411582	−77.344776	−77.335364	−77.329808	−77.328491
MP2	−77.653128	−77.585437	−77.575371	−77.574170	−77.585551
MP3	−77.677132	−77.608638	−77.597405	−77.594164	−77.601643
MP4SDQ	−77.682922	−77.617077	−77.606085	−77.602606	−77.608729
MP4SDTQ	−77.690946		−77.615673	−77.612981	−77.620639
PUHF	−77.424365	−77.368966	−77.361912	−77.354353	−77.343418
PMP2	−77.664614	−77.606834	−77.598892	−77.595836	−77.598452
PMP3	−77.686371	−77.625632	−77.616158	−77.611205	−77.611209
PMP4SDQ	−77.692161	−77.634071	−77.624838	−77.619647	−77.618295
PMP4SDTQ	−77.700185		−77.634426	−77.630022	−77.630205
Spin					
$\langle\Psi_0\|S^2\|\Psi_0\rangle$	0.9905	1.1419	1.1858	1.1458	0.9659
$\langle\Psi_0\|S^2\|\Psi_0 + \Psi_1\rangle$	0.9655	1.0938	1.1329	1.0968	0.9358
$\langle\Psi_0\|S^2\|\Psi_0 + \Psi_1 + \Psi_2\rangle$	0.9228	1.0184	1.0498	1.0184	0.8864
Relative energies[a] (kcal/mol)					
HF	−38.45	−2.03	3.32	6.30	7.11
MP2	−21.95	15.03	20.78	21.04	13.88
MP3	−30.34	7.14	13.63	15.17	10.45
MP4SDQ	−31.25	4.57	10.91	12.59	8.73
MP4SDTQ	−27.91		13.27	14.46	9.63
PUHF	−46.47	−17.21	−13.34	−9.10	−2.26
PMP2	−29.16	1.60	6.02	7.44	5.78
PMP3	−36.13	−3.52	1.86	4.47	4.45
PMP4SDQ	−37.04	−6.09	−0.86	1.90	2.73
PMP4SDTQ	−33.71		1.50	3.76	3.63

[a]Includes zero point energy calculated at the UHF/6-31G* level, see Table I.

2.0000	2.1000	2.2000	2.3000	2.5000	2.7000	infinite
1.1953	1.1897	1.1866	1.1848	1.1832	1.1826	1.1823
1.0558	1.0551	1.0549	1.0549	1.0551	1.0551	1.0556
1.0558	1.0556	1.0556	1.0556	1.0556	1.0556	1.0556
106.81	105.95	105.76	105.50	105.75	106.08	—
169.05	172.82	174.96	176.50	178.16	178.93	180.00
175.55	177.22	177.90	178.73	179.26	179.57	180.00
−77.329639	−77.331371	−77.333141	−77.334742	−77.337222	−77.338830	−77.341048
−77.593350	−77.597582	−77.600640	−77.602896	−77.605747	−77.607276	−77.608890
−77.606829	−77.609903	−77.612276	−77.614116	−77.616573	−77.617967	−77.619528
−77.612700	−77.615178	−77.617183	−77.618787	−77.621022	−77.622338	−77.623871
−77.625433	−77.628230					−77.637213
−77.337511	−77.336084	−77.335984	−77.336434	−77.337824	−77.339045	−77.341048
−77.600085	−77.601598	−77.603055	−77.604329	−77.606252	−77.607455	−77.608890
−77.611647	−77.612732	−77.613962	−77.615110	−77.616921	−77.618090	−77.619528
−77.617518	−77.618007	−77.618869	−77.619781	−77.621370	−77.622461	−77.623871
−77.630251	−77.631059					−77.637213
0.8601	0.8154	0.7892	0.7731	0.7579	0.7527	0.7500
0.8440	0.8056	0.7833	0.7695	0.7567	0.7522	0.7500
0.8169	0.7891	0.7732	0.7635	0.7546	0.7521	0.7500
6.83	5.93	4.92	4.00	2.42	1.41	0.00
9.42	6.96	5.14	3.80	1.99	1.03	0.00
7.64	5.90	4.51	3.44	1.87	1.00	0.00
6.68	5.31	4.16	3.23	1.81	0.98	0.00
7.06	5.50					0.00
1.89	2.97	3.14	2.94	2.04	1.28	0.00
5.20	4.44	3.62	2.90	1.68	0.92	0.00
4.62	4.12	3.45	2.81	1.66	0.92	0.00
3.66	3.54	3.10	2.61	1.59	0.90	0.00
4.04	3.72					0.00

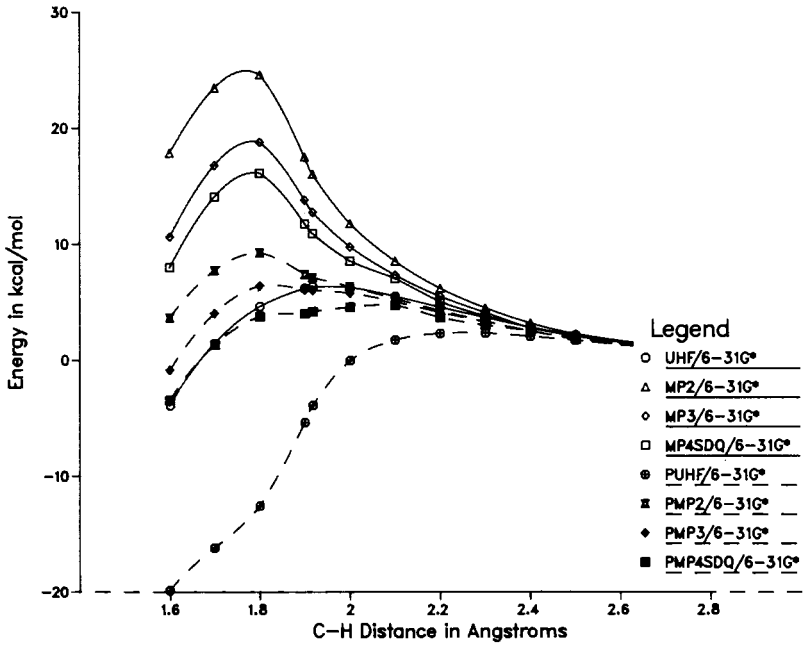

Figure 3. The potential energy curve along the approximate reaction path for H + $C_2H_2 \rightarrow C_2H_3$ without spin projection (solid lines) and with spin projection (dashed lines) using the 6-31G* basis set.

ments in the calculations could cause additional changes in the location of the transition state. The heat of reaction at the PMP4SDTQ/6-311G** level is $\Delta H(298\ \text{K}) = -34.4$ kcal/mol, in very good agreement with the experimental estimate [11] and the BAC-MP4 calculations [12].

Table IV lists the results of the MP*n*/6-31G* and PMP*n*/6-31G* grid search for transition state geometries. The trends are the same as those deduced from the potential energy profiles along the reaction path. At the MP*n* levels, R(CH*) is 0.2–0.3 Å shorter than the Hartree–Fock optimized value. The MP*n* barriers estimated from the grid search are somewhat lower than those obtained from the reaction path energy profiles but are still too high by 10–15 kcal/mol relative to experimental barrier. With spin projection, the barriers are much lower and are in good agreement with the barrier heights estimated from the potential energy profiles. Compared with the MP*n* calculations, spin projection shifts the barriers by 0.15–0.2 Å toward H + C_2H_2, also in good agreement with the data obtained from Table I and Figure 3.

Vibrational frequencies were calculated at the UHF/6-31G* level for a number of the points along the approximate reaction path (see Table I and Fig. 6). The labels for the vibrational modes correspond to the reactants. From the reactants to the transition structure, the zero point energy changes by −0.7 kcal/mol, because of a large

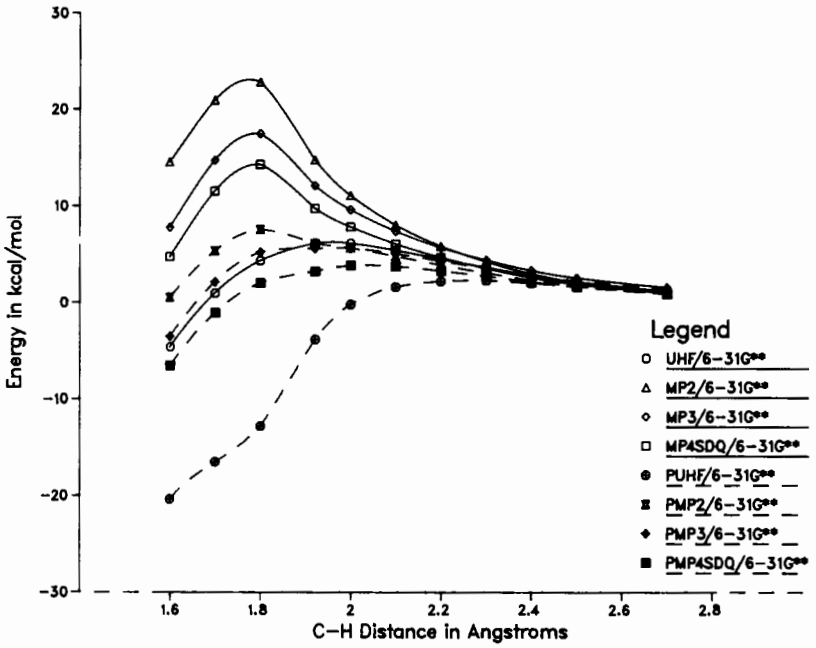

Figure 4. The potential energy curve along the approximate reaction path for H + $C_2H_2 \rightarrow C_2H_3$ without spin projection (solid lines) and with spin projection (dashed lines) using the 6-31G** basis set.

decrease in the C — C stretching frequency as well as smaller decreases in the other acetylene frequencies; the CCH* bend is still relatively low in frequency, and the CH* stretching frequency is imaginary. Based on the grid search calculations, the

TABLE IV. Geometries and barrier heights for H + HCCH estimated from a grid search with the 6-31G* basis set.

	MP2	MP3	MP4SDQ	MP4SDTQ	PMP2	PMP3	PMP4SDQ	PMP4SDTQ
Geometrical parameters[a] (Å and degrees)								
R(CH*)	1.62	1.73	1.76	1.72	1.81	1.88	1.91	1.87
R(CC)	1.202	1.203	1.210	1.211	1.217	1.216	1.224	1.224
<CCH*	111.7	111.1	111.5	111.8	110.9	110.3	110.7	110.9
$<CCH_1$	157.0	159.0	158.4	157.6	159.4	160.2	159.4	159.1
$<CCH_2$	165.1	167.4	166.6	165.3	170.2	169.9	168.2	168.4
Estimated barrier[b] (kcal/mol)								
	19.0	14.0	12.5	14.5	8.5	6.5	5.0	6.5

[a]R(CH1) and R(CH2) fixed at 1.06955 Å (MP4/6-31G* optimized bond length in C_2H_2); estimated errors due to the grid search: ±2° for angles, ±0.005 Å for R(CC), ±0.05 Å for R(CH*), and ±0.5 kcal/mol for the barrier height.

[b]Includes zero point energy calculated at the UHF/6-31G* level.

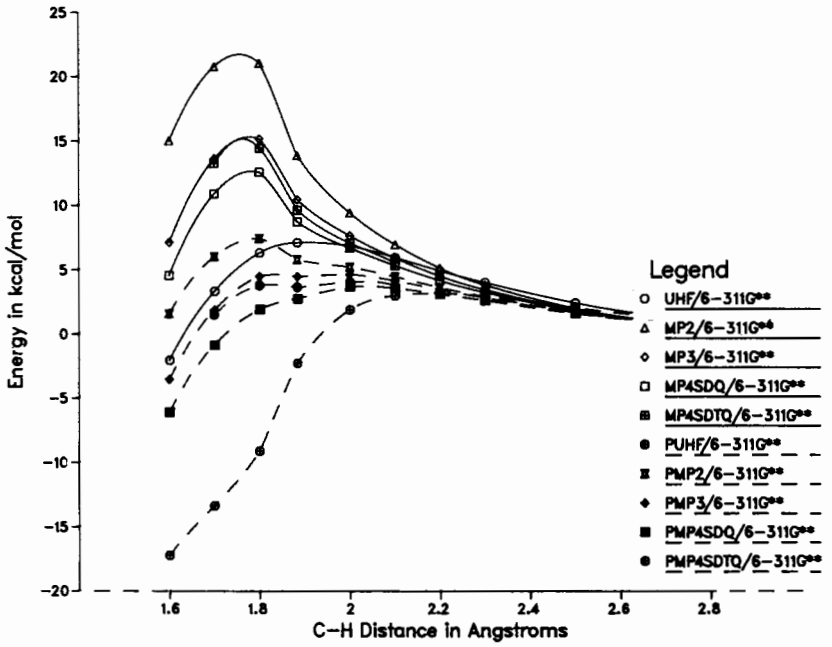

Figure 5. The potential energy curve along the approximate reaction path for H + $C_2H_2 \rightarrow C_2H_3$ without spin projection (solid lines) and with spin projection (dashed lines) using the 6-311G** basis set.

decrease in the C — C stretching force constant at the transition state appears to be much smaller when correlation and spin corrections are included. This suggests that the frequencies and changes in the zero point energies calculated at the POL-CI level [10] may be more realistic. From the transition structure to the products, the zero point energy increases by 6.5 kcal/mol, primarily because of the CH* stretching mode. The thermodynamic parameters obtained at the UHF/6-31G* level were also used for the calculations with the larger basis sets.

In canonical variational transition state theory, the position of the activated complex is chosen to be at the maximum in $\Delta E^{\ddagger}(0\ \mathrm{K}) + RT \ln Q^{\ddagger}$ along the reaction path [28]. For H + C_2H_2, $\ln Q^{\ddagger}$ is almost constant in the region of the transition state, and the position of the variational transition state is essentially the same as the vibrationally adiabatic barrier. At $T = 298$ K, the activation energy for the cannonical variational transition state is $E_a = 4.3$ kcal/mol. This is significantly lower than previous calculations at the POL-CI level [10] but still 1.6–1.9 kcal/mol higher than the experimental activation energy of 2.4–2.7 kcal/mol [1–3]. The calculated preexponential factor, $A = 1.48 \times 10^{10}$ l/mol s, is in good agreement with the experimental range of values, $0.5–2.2 \times 10^{10}$ l/mol s [1–3].

Conclusions

Spin projection can cause important changes in the height, shape, and position of the barriers of reactions in which the transition state has significant spin contamina-

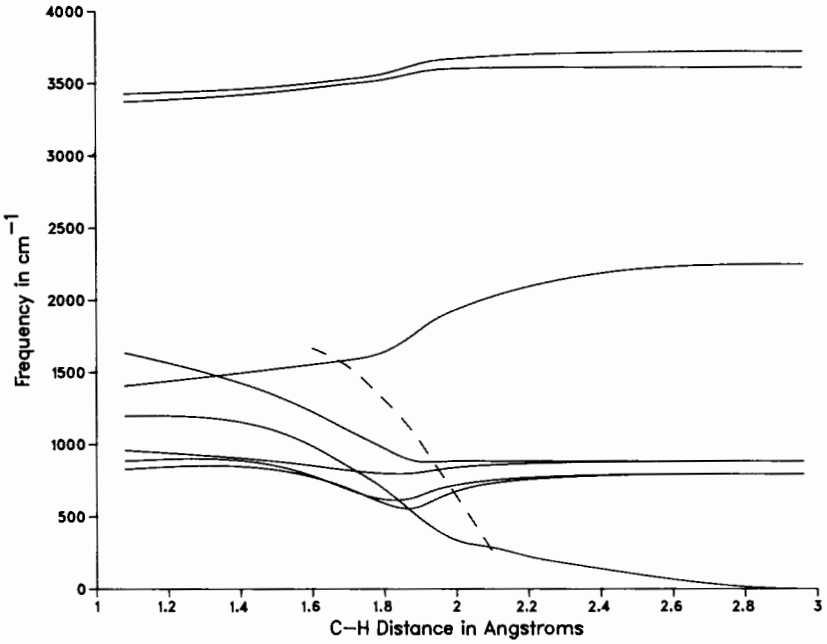

Figure 6. Variation of the vibrational frequencies along the approximate reaction path for $H + C_2H_2 \rightarrow C_2H_3$ (6-31G* basis set).

tion. For $H + C_2H_2$ addition, spin projection lowers the UMP*n* barrier by 10–20 kcal/mol and shifts it toward the reactants. The agreement with the experimental activation energy is significantly improved.

Acknowledgment

This work was supported by a grant from the National Science Foundation (CHE-83-12505).

Bibliography

[1] W. A. Payne and L. J. Stief, *J. Chem. Phys.* **64**, 1150 (1976).
[2] K. Sugawara, K. Okazaki, and S. Sato, *Bull. Chem. Soc. Jpn.* **54**, 2872 (1981).
[3] R. Ellul, P. Potzinger, B. Reimann, and P. Camilleri, *Ber. Bunsenges. Phys. Chem.* **85**, 407 (1981).
[4] D. G. Keil, K. P. Lynch, J. A. Cowfer, and J. V. Michael, *Int. J. Chem. Kinet.* **8**, 825 (1976).
[5] J. H. Lee, J. V. Michael, W. A. Payne, and L. J. Stief, *J. Chem. Phys.* **68**, 1817 (1978).
[6] W. L. Hase, R. J. Wolfe, and C. S. Sloane, *J. Chem. Phys.* **71**, 2911 (1979); W. L. Hase and D. G. Buckowski, *J. Comp. Chem.* **3**, 335 (1982).
[7] S. Nagase, and C. W. Kern, *J. Am. Chem. Soc.* **101**, 2544 (1979).
[8] D. J. Hucknall, *Chemistry of Hydrocarbon Combustion* (Chapman and Hall, New York, 1985).
[9] J. Warnatz, in *Combustion Chemistry*, W. C. Gardiner Jr., Ed. (Springer-Verlag, New York, 1984), p. 197.
[10] L. B. Harding, A. F. Wagner, J. M. Bowman, G. C. Schatz, and K. Christoffel, *J. Phys. Chem.* **86**, 4312 (1982).

[11] S. Benson, *Thermochemical Kinetics* (John Wiley & Sons, New York, 1976).
[12] C. Melius and J. S. Binkley, to be published.
[13] C. Sosa and H. B. Schlegel, *Int. J. Quantum Chem.* **29**, 1001 (1986); **30**, 155 (1986).
[14] C. Sosa and H. B. Schlegel, *J. Am. Chem. Soc.* **109**, 4193 (1987).
[15] N. C. Handy, P. J. Knowles, and K. Somasundram, Theor. Chim. Acta, **68**, 87 (1985); P. J. Knowles, K. Somasundram, N. C. Handy, and K. Hirao, *Chem. Phys. Lett.*, **113**, 8 (1985).
[16] W. D. Laidig, G. Fitzgerald, and R. J. Bartlett, *Chem. Phys. Lett.* **113**, 151 (1985).
[17] P. M. W. Gill and L. Radom, *Chem. Phys. Lett.* **132**, 16 (1986).
[18] H. B. Schlegel, *J. Chem. Phys.* **84**, 4530 (1986).
[19] J. S. Binkley, R. A. Whiteside, R. Krishnan, R. Seeger, D. J. DeFrees, H. B. Schlegel, S. Topiol, L. R. Kahn, and J. A. Pople, GAUSSIAN 80. *QCPE* **13**, 406 (1980); J. S. Binkley, M. J. Frisch, D. J. DeFrees, K. Raghavachari, R. A. Whiteside, R. Seeger, H. B. Schlegel, and J. A. Pople, GAUSSIAN 82, Carnegie-Mellon University, Pittsburgh, Pa., 1983.
[20] W. J. Hehre, R. Ditchfield, and J. A. Pople, *J. Chem. Phys.* **56**, 2257 (1972); P. C. Hariharan, and J. A. Pople, *Chem. Phys. Lett.* **66**, 217 (1972); R. Krishnan, J. S. Binkley, R. Seeger, and J. A. Pople, *J. Chem. Phys.* **72**, 650 (1980).
[21] C. Møller, and M. S. Plesset, *Phys. Rev.* **46**, 618 (1934).
[22] R. J. Bartlett, *Ann. Rev. Phys. Chem.* **32**, 359 (1981).
[23] H. B. Schlegel, J. Comput. Chem. **3**, 214 (1982).
[24] D. J. DeFrees, J. S. Binkley, A. D. McLean, *J. Chem. Phys.* **80**, 3720 (1984).
[25] P.-O. Löwdin, *Phys. Rev.* **97**, 1509 (1955).
[26] J. A. Pople, R. Krishnan, H. B. Schlegel, and J. S. Binkley, *Int. J. Quantum. Chem., Quantum Chem. Symp.* **13**, 225 (1979).
[27] D. A. McQuarrie, *Statistical Thermodynamics* (Harper & Row, New York, 1973).
[28] D. G. Truhlar, and B. C. Garrett, *Acc. Chem. Res.* **13**, 440 (1980).

Received June 15, 1987